

Refractive index spectral dependence, Raman and transmission spectra of high-purity ^{28}Si , ^{29}Si , ^{30}Si , and $^{\text{nat}}\text{Si}$ single crystals

V.G.Plotnichenko,* V.O.Nazaryants, E.B.Kryukova, V.V.Koltashev, V.O.Sokolov, and E.M.Dianov
Fiber Optics Research Center of the Russian Academy of Sciences
38 Vavilov Street, Moscow 119333, Russia

A.V.Gusev, V.A.Gavva, T.V.Kotereva, and M.F.Churbanov
Institute of Chemistry of High-Purity Substances of the Russian Academy of Sciences
49 Tropinin Street, Nizhny Novgorod 603600, Russia

Precise measurement of the refractive index of stable silicon isotopes ^{28}Si , ^{29}Si , ^{30}Si single crystals with enrichments above 99.9 at.% and a silicon single crystal $^{\text{nat}}\text{Si}$ of natural isotopic composition is performed with the Fourier-transform interference refractometry method from 1.06 to more than 80 μm with 0.1 cm^{-1} resolution and accuracy of $2 \times 10^{-5} \dots 1 \times 10^{-4}$. The oxygen and carbon concentrations in all crystals are within $5 \times 10^{15} \text{ cm}^{-3}$ and the content of metal impurities is $10^{-5} \dots 10^{-6}$ at.%. The peculiar changes of the refractive index in the phonon absorption region of all silicon single crystals are shown. The coefficients of generalized Cauchy dispersion function approximating the experimental refractive index values all over the measuring range are given. The transmission and Raman spectra are also studied.

I. INTRODUCTION

Production and study of the properties of isotopically enriched substances are one of the crucial problems of contemporary material science involving in itself the increasing number of researchers. Owing to the achieved level of purity of many substances, their properties are substantially determined by the isotopic composition.

Development of the technology of high-purity monoisotopic single crystals production allows one to study the influence of the isotopic composition on physical properties, in particular on the electronic, phonon, and Raman spectra and the refractive index dispersion. This is important both for verification of existing theoretical models and filling them with more correct values of used parameters, and for calculation of parameters of next-generation devices developed on their basis.

Crystalline silicon is known to be the basic material of microelectronics and solar energetics. Besides, it is also an attractive optical material with high transmission in the near- to mid-IR spectral range. In recent years silicon photonics grows rapidly, which is expected to find application in future optical fiber communication and information transfer systems. Monoisotopic silicon is considered to be the basic component of quantum computers [1].

Formerly silicon refractive index was measured repeatedly in various spectrum ranges by many laboratories and companies (see e.g. [17–21]). The papers [17, 18] seem to be the first in this field. The analysis of more than 50 papers made in 1980 [19] showed the data available to be scattered widely, but allowed to derive certain averaged spectral dependence for silicon refractive index which is rather often referred to. Unfortunately, in the

majority of published papers devoted to silicon refractive index measuring, the crystals used for this purpose are characterized neither in purity, nor in conductivity, both influencing the measurement results.

In this paper we present the results of measuring the room-temperature transmission spectra in the short-wavelength edge and phonon absorption regions, the Raman spectra excited by the 514.5 nm Ar laser line and the refractive index spectral dependence in the near-, mid-, and far-IR spectral ranges in silicon single crystals with natural isotopic composition, $^{\text{nat}}\text{Si}$, and silicon isotopes ^{28}Si , ^{29}Si , ^{30}Si with the basic isotope content above 99.9 at.% prepared by the same technology. A short note on fabrication of these single crystals and refractive index measurements in the 1.06...25.5 μm range has been published recently [2].

II. PREPARATION OF SINGLE CRYSTALS AND SAMPLES FOR MEASUREMENTS

Polycrystalline silicon was prepared by thermal decomposition of monosilane enriched in one of the silicon isotopes as described in [3, 4]. The decomposition was proceed on a graphite substrate surface at 800 °C. After a few mm thick layer was deposited, polycrystalline silicon was separated from the graphite substrate, remelted to form a rod, and purified by 10 float zoning passes. Then this monoisotopic silicon rod was used as a substrate to deposit the polycrystalline silicon layer till an ingot of a required diameter was obtained.

To minimize the effect of isotopic dilution by a seedling material, a special growth procedure [5] was used. Preliminarily a single-crystal seed with the isotopic composition gradient in length was grown by drawing at the end of mono-isotopic silicon ingot of a cylindrical site with a diameter not exceeding that of a seed from sili-

* E-mail: victor@fo.gpi.ac.ru

Table I: Results of mass spectrometry determination of isotopic composition of produced Si single crystals

Single crystal	Isotopic composition, at.%		
	^{28}Si	^{29}Si	^{30}Si
^{28}Si	99.9934	0.00637	0.00023
^{29}Si	0.026	99.919	0.055
^{30}Si	0.005	0.021	99.974

con of natural isotopic composition. The composition of grown single crystal seed was almost identical to the isotopic composition of polycrystalline ingot which the single crystal was grown from. Single crystals were grown in the [100] direction by float zoning in a high-purity argon atmosphere. The same procedure was used to prepare a single crystal of natural isotopic composition, $^{\text{nat}}\text{Si}$: ^{28}Si (92.23%), ^{29}Si (4.68%), and ^{30}Si (3.09%) [6].

The isotopic composition of the crystals was determined by mass spectrometry [7] with an accuracy better than 0.01 at.% (Table I). Comparison with the data reported in [8, 9] indicates that our crystals are more isotopically enriched and offer higher chemical purity and resistivity.

Structural perfection of the crystals was evaluated using X-ray diffraction and selective etching. No orientation disorder, low-angle boundaries or twinning regions were detected in the single crystals grown. The half-width of their rocking curves was $11 \dots 12''$. The room-temperature resistivity of the crystals was found to be $100\text{--}200 \Omega \times \text{cm}$. According to mass spectrometric measurements, the contents of 72 impurities was below the mass spectrometry detection limit ($\lesssim 10^{-5} \dots 10^{-6}$ at.%) [10].

2...3 mm-thick plates were cut perpendicularly to the growth axis of the cylindrical samples prepared. Then the plates were ground and polished with various flatness degrees for measuring the transmission spectra without interference at 2 cm^{-1} resolution (to analyze the presence of impurity absorption bands and intrinsic bands shift in the two-phonon absorption range) and with interference at 0.1 cm^{-1} resolution (to measure the refractive index spectral dependence). Samples for the refractive index measurements had the surface flatness better than 1/10 of Newton's fringe ($\lambda = 546 \text{ nm}$), parallelism of sides better than $1''$, and the surface finish class of 60/40.

III. TRANSMISSION SPECTRA

The transmission spectra of crystalline silicon without interference were measured on Lambda 900 spectrophotometer in a short-wavelength range ($0.9 \dots 1.6 \mu\text{m}$) and on Bruker IFS-113v Fourier-transform vacuum spectrometer in a longer wavelength range ($1 \dots 90 \mu\text{m}$). The analysis on the presence of impurity absorption bands in the transmission spectra measured in conformity with

the ASTM standards F-1188 and F-1391 [11] proved oxygen and carbon contents to be less than $5 \times 10^{15} \text{ cm}^{-3}$ in all the samples under investigation.

In the 1 to 3 mm thickness crystals the tendency to the transmission edge shift to higher frequencies with isotope atomic mass increasing was observed in the short-wavelength transmission edge region at room temperature. However, the shift value of $\lesssim 1 \text{ meV/a.m.u.}$ was comparable with the experimental error.

The $M^{-1/2}$ dependence of the band gap, E_g , was shown in [12] to be more probable for $T < 50 \text{ K}$, since due to lattice expansion and electron-phonon interaction E_g decreases linearly with T growing in the room-temperature region ($\sim 294 \text{ K}$). Measurement at 16 K of the transmission spectra of our silicon samples showed that with atomic mass increasing the absorption edge shifts to the high-energy region. The shift was found to be $\mp (1.8 \pm 0.3) \text{ meV}$ in ^{28}Si and ^{30}Si relative to ^{29}Si . The indirect transition energy determined from the optical absorption edge was found to depend on the average atomic mass as $M^{-1/2}$. The shift $\sim 1.5 \text{ meV}$ measured in the present work at 16 K turned out to be somewhat higher compared with 1 meV derived from the luminescence spectra in [12].

In the phonon absorption region ($5 \dots 30 \mu\text{m}$) a shift of all absorption bands to longer wavelengths was observed, which had been seen previously in isotopically enriched silicon single-crystal samples with a smaller isotopic enrichment [13].

IV. RAMAN SPECTRA

The Raman spectra of all produced single crystals were measured on a T64000 triple spectrograph in a backscattering geometry at room temperature. The 514.5-nm argon laser line was used as an incident radiation. The scattered radiation was detected by a liquid nitrogen-cooled CCD matrix. The spectra were gathered in 0.7 cm^{-1} steps. Spectrograph was calibrated using radiation in Ar laser and Hg lamp lines.

The Raman band corresponding to first-order scattering by Γ_{15} symmetry phonons was observed in spectra of all the single crystals (showed as circles in Fig. 1a). The band turned out to be well fitted by a Lorentzian with width $3.3 \dots 3.4 \text{ cm}^{-1}$ for ^{28}Si , ^{29}Si , ^{30}Si and 3.7 cm^{-1} for $^{\text{nat}}\text{Si}$ (solid lines in Fig. 1a). This is an evidence of high structural perfection of the mono-isotopic single-crystal samples.

The peak position, Ω , of this Raman band is plotted vs. atomic mass, M_i , in Fig. 1b for all silicon single crystals. The dashed line represents the best fit of the experimental phonon frequency values for all the single-crystal samples by the $\Omega = 2731.9 (M_i [\text{a.m.u.}]^{-1/2} \text{ cm}^{-1})$ dependence valid in harmonic approximation. The root-mean-square deviation, SD , of experimental Ω points from the fitted line turned out to be small for the mono-isotopic samples. Again this is an indirect evidence of high struc-

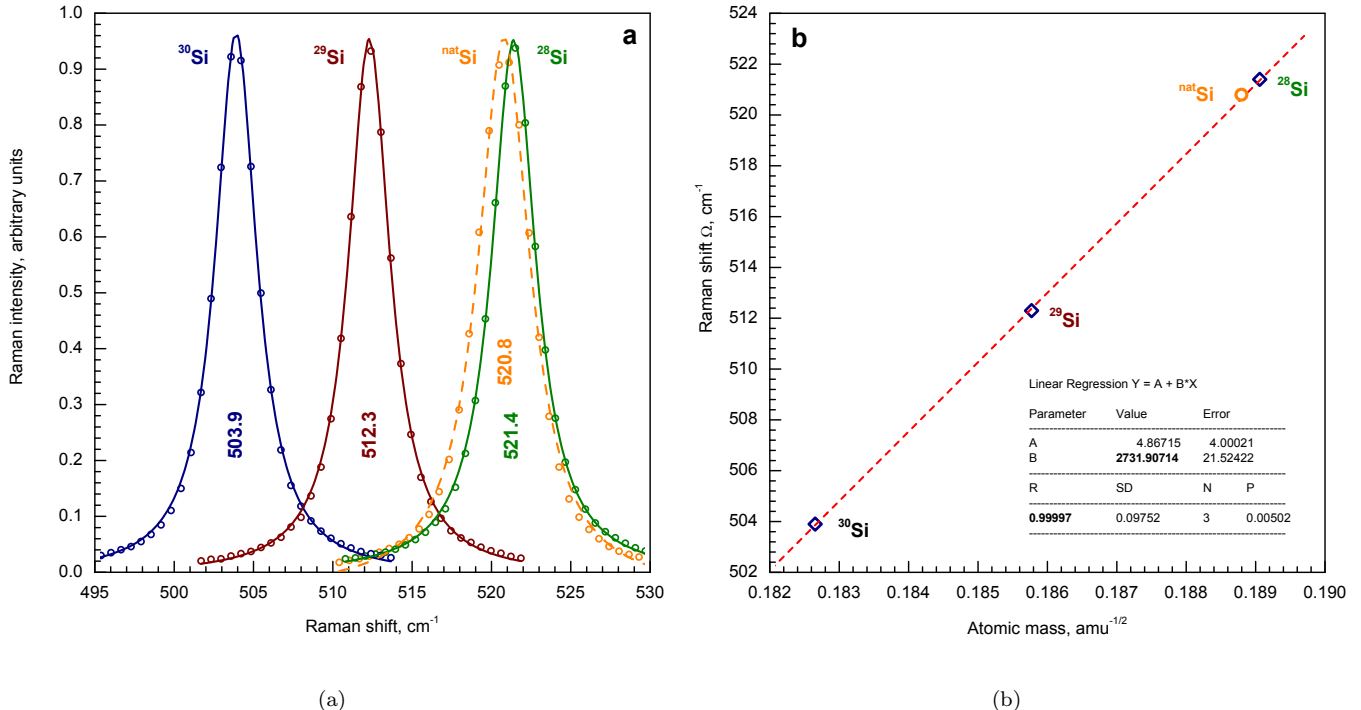


Figure 1: (a) Fundamental Raman band of ²⁸Si, ²⁹Si, ³⁰Si, and ^{nat}Si (natural isotopic composition) single crystals. (b) Peak position Ω of the Raman band vs. isotopic crystal composition

tural perfection of those. The Raman band peak position for ^{nat}Si sample falls slightly above the fitted line, the band being wider than in mono-isotopic samples. This is attributable to both anharmonicity related to different atomic masses of isotopes and to worse structural perfection of ^{nat}Si crystal in comparison with the mono-isotopic ones (see further).

V. REFRACTIVE INDEX

A. Measurements

To measure refractive index we used the improved method of interference refractometry [14–16]. In this method firstly the order, m , of the interference maximum is determined with the absolute accuracy from the peak position, ν_m , in the interference transmission spectra of plane-parallel plates cut from the studied material, and then the refractive index value, $n(\nu_m)$, is calculated all over the interference transmission range measured using the expression

$$2h n(\nu_m) \nu_m = m \quad (1)$$

The measurements were performed for plane-parallel plates of three thicknesses (from 0.8 to 1.2 mm) cut from silicon samples of all the isotope compositions using Bruker IFS-113v Fourier-transform vacuum spectrometer in 9500...110 cm⁻¹ wavenumber range (1.05...90 μ m

wavelength range) with 0.1 cm⁻¹ resolution. The diameter of a radiation beam transmitted through the samples did not exceed 3 mm. At least twenty data points were obtained for each interference maximum. The plates thickness was measured on DG-30 holographic submicrometer with the accuracy better than 0.05 μ m. During transmission spectra and thickness measurements sample temperature was hold to be 21.2 ± 0.05 °C.

Fig. 2 shows the refractive index spectral dependences over the entire measurement range for all the single crystal samples studied. As well the most frequently cited literature data for silicon single crystals with a natural isotopic composition [17–21] are shown. As evident from Fig. 2, the scatter of the refractive index data for silicon with a natural isotopic composition exceeds considerably the difference in the refractive index values of mono-isotopic silicon single crystals.

With silicon isotope atomic mass increasing, the refractive index spectral dependences measured by us far from electron and phonon transition edges shifts downwards. As an example, the refractive index values of the silicon single crystals are listed in Table II for 1.5, 2 and 5 μ m wavelengths.

It is known that two-phonon lattice absorption bands at 16.4 μ m (610 cm⁻¹) with the maximum intensity of 9 cm⁻¹ are observable in the 6.7...20 μ m (1500...500 cm⁻¹) spectral range in the spectra of 1...2 mm-thick silicon samples. According to [22], those should give rise to well-distinguished features in the re-

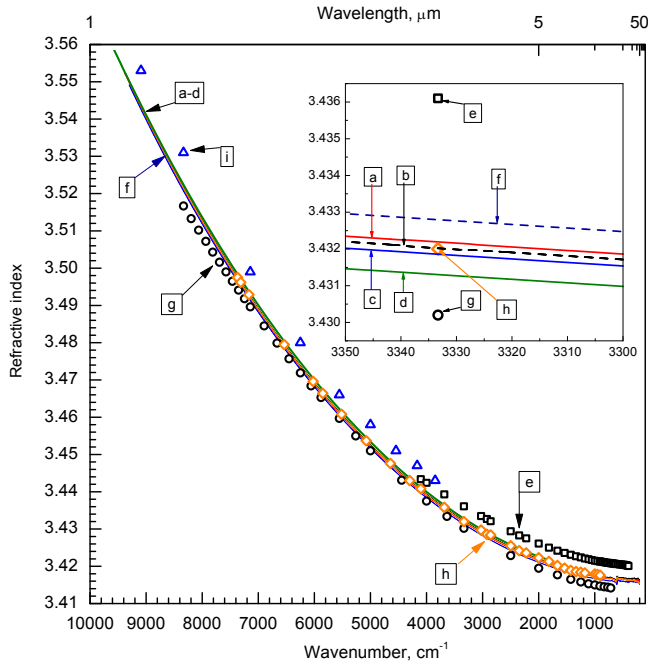


Figure 2: Spectral dependence of the refractive index: our measurements for silicon samples (a) ^{28}Si , (b) $^{\text{nat}}\text{Si}$, (c) ^{29}Si , (d) ^{30}Si ; the literature data for silicon crystals with natural isotopic composition (i) [17], (h) [18], (g) [19], (e) [20], (f) [21].

Table II: Refractive index values of silicon single crystals at the wavelengths 1.5, 2, and 5 μm

Single crystal	1.5 μm	2 μm	5 μm
^{28}Si	3.48207	3.45260	3.42194
$^{\text{nat}}\text{Si}$	3.48191	3.45243	3.42177
^{29}Si	3.48171	3.45224	3.42161
^{30}Si	3.48112	3.45168	3.42107

fractive index dispersion. The transmission spectra measured with 2 cm^{-1} resolution for all 1.2 mm-thick silicon crystals are shown in Fig. 3 (a). Fig. 3 (b) presents the variation of the crystals refractive index measured by us in this spectral region. The absorption band shift to longer wavelengths with silicon isotope atomic mass increasing and the anomalous behavior of refractive index dispersion well-conforming to the classic Lorentz theory are clearly seen. As far as we know, we managed to observe such a refractive index spectral behavior in the region of so low absorption (less than 10 cm^{-1}) for the first time. For example, in [20] (line e in Fig. 2) the interference refractometry method was used as well to measure the refractive index of n-type silicon (phosphorus-doped with $3 \dots 4\ \Omega \times \text{cm}$ resistivity) in $2.43 \dots 25\ \mu\text{m}$ wavelength range at $26\text{ }^\circ\text{C}$. However, no peculiarities in the two-phonon absorption region were revealed. In the first

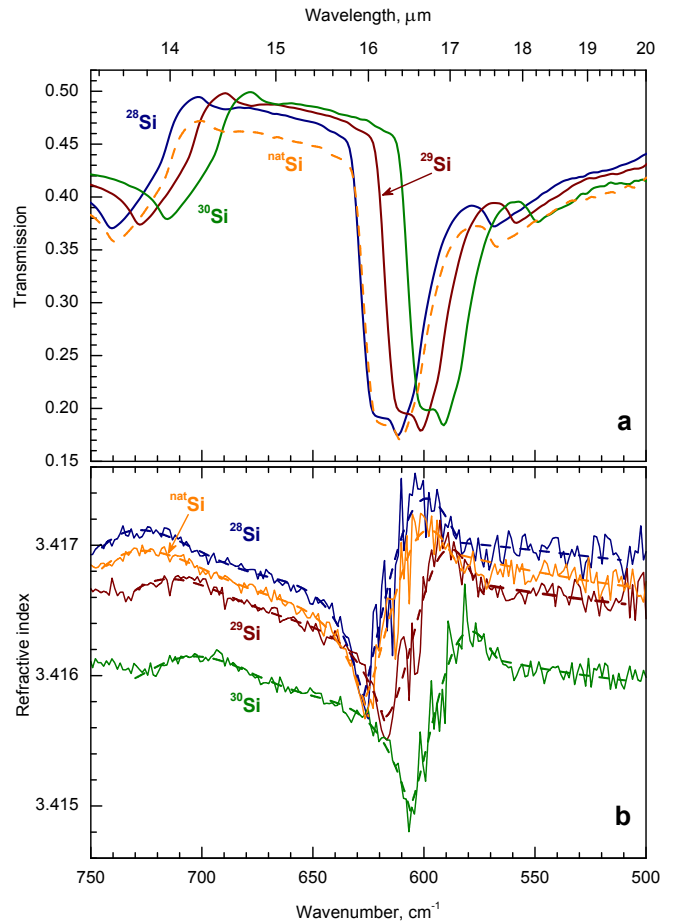


Figure 3: (a) Transmission spectral dependence of for 1.2-mm thick ^{28}Si , ^{29}Si , ^{30}Si , and $^{\text{nat}}\text{Si}$ samples in the IR region of phonon absorption peak. (b) Refractive index spectral dependence of the same single crystals.

approximation, the uncertainty in the refractive index values was attributed by the authors of [20] to the uncertainty in sample thickness (1 part per 10^4), which, in our opinion, is quite enough to observe the changes in the spectral dependence of silicon refractive index shown in Fig.3 (b).

The refractive index values calculated from the transmission spectra are conventionally approximated by analytical formulas allowing one to preserve the experimental accuracy of refractive index determination. The Sellmeier or Herzberger formulas are often used to approximate the refractive index spectral dependence. However, our studies show that the application of generalized Cauchy dispersion function [23] allows us to reduce the root-mean-square deviation of the approximation from the calculated refractive index values by several times. Therefore we used it to fit the experimental data:

$$n(\nu) = \sum_{i=1}^5 (A_{2i} \nu^{2i} + B_{2i} \nu^{-2i}) + C \quad (2)$$

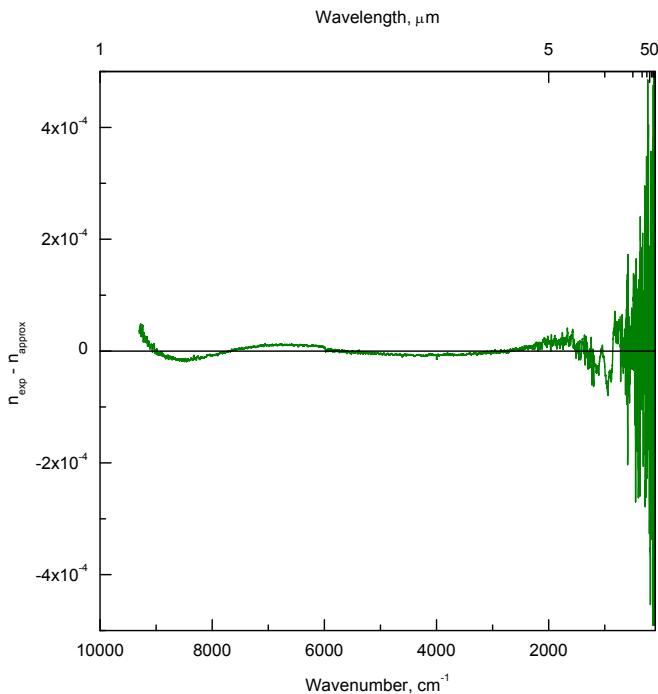


Figure 4: Spectral dependence of the difference between the calculated, n_{exp} , and approximated, n_{approx} , refractive index for ^{30}Si single crystal.

Here ν is the wavenumber, $\nu [\text{cm}^{-1}] = 10^4 \times \lambda^{-1} [\mu\text{m}]$.

Due to the presence of phonon absorption lines, the range of refractive index approximation was subdivided into four parts. This allowed us to reduce considerably the root-mean-square deviation between the measured and approximated refractive index values and to bring it to the level not exceeding 1×10^{-4} . The coefficients of Cauchy approximation (2) for refractive index of all silicon single crystals corresponding to the best fit to the experimental results, are given in Tables III–VI. The values of mean-square deviation for all approximation

$$E_g(T, M_i) = E_B - a_B \left(\frac{M_{\text{nat}}}{M_i} \right)^{1/2} \left[1 + \frac{2}{\exp(\Omega(M_i)/T) - 1} \right]$$

$$\Omega(M_i) = \Omega_0 \left(\frac{M_{\text{nat}}}{M_i} \right)^{1/2}$$

where M_{nat} is the average atomic mass of natural silicon, $\{\exp(\Omega(M_i)/T) - 1\}^{-1}$ is phonon Bose distribution function, Ω_0 is the model parameter. According to [27], $E_B \approx 28713.3 \text{ cm}^{-1}$, $a_B \approx 967.9 \text{ cm}^{-1}$.

The oscillator parameters, α_i and β_i , depend on isotopic composition as well. First, both parameters depend on the lattice constant as a_0^{-3} and a_0 is known to change with isotopic composition (see e.g. [29]). However, this

dependence is negligible in the qualitative model under consideration. Second, in the case of silicon the phonon-related parameter, β_i , describes the IR absorption due to two-phonon transitions and hence depends on the atomic mass as $\beta_i \sim M_i^{-2}$ [30]. Therefore

$$\alpha_i = \alpha_0$$

$$\beta_i = \beta_0 M_i^{-2}$$

ranges are listed at the foot of the tables. As an example, the spectral dependence of the difference between the calculated refractive index for ^{30}Si single crystal and its approximated values is shown in Fig. 4. It is seen that the deviation of the approximation from the calculated refractive index values does not exceed 5×10^{-5} in a sufficiently wide range. However, with the wavelength exceeding $16 \mu\text{m}$ the accuracy of peak position determination decreases owing to noticeable growth of noise in the transmission spectra. Accordingly, the accuracy of the refractive index calculation is reduced.

Comparing our results to the data published, we found that the refractive index values closest to ours for natural silicon are given in [21]. In that work measurements were carried out by the prism method with 1×10^{-4} relative accuracy at several wavelengths in the $1.1 \dots 5.5 \mu\text{m}$ range at temperature from 20 to 300 K. The results obtained were approximated by the Sellmeier formula.

B. On the origin of the dispersion curve shift

The observed shift of the dispersion curve is easily understood using classic models of a lattice of oscillators with dipolar coupling [24, 25]. Neglecting the spatial dispersion the dielectric constant of a cubic lattice is expressed in this model by the equation

$$\varepsilon(\omega) = 1 - \frac{\alpha_i E_g(M_i)}{\omega^2 - E_g^2(M_i)} - \frac{\beta_i \Omega(M_i)}{\omega^2 - \Omega^2(M_i)}$$

where M_i is the atomic mass of ^iSi isotope, $E_g(M_i)$ is the band gap (fundamental absorption short-wavelength edge energy), $\Omega(M_i)$ is the phonon frequency (fundamental absorption long-wavelength edge energy), α_i and β_i are the model parameters representing two types of oscillators corresponding to the electron and phonon fundamental absorption edges, respectively. With no absorption, the refractive index equals to $n(\omega) = \varepsilon^{1/2}(\omega)$.

The fundamental absorption edge energies depend on isotopic composition and for an isotopically pure crystal can be expressed as [26–28]:

dependence is negligible in the qualitative model under consideration. Second, in the case of silicon the phonon-related parameter, β_i , describes the IR absorption due to two-phonon transitions and hence depends on the atomic mass as $\beta_i \sim M_i^{-2}$ [30]. Therefore

Table III: Parameters of the approximation of ^{28}Si single crystal refractive index

Parameter	Spectral range			
	9400...745 cm^{-1} (1.06...13.42 μm)	745...625 cm^{-1} (13.42...16.00 μm)	625...583 cm^{-1} (16.00...17.15 μm)	583...117 cm^{-1} (17.15...85.47 μm)
A_6	4.03488×10^{-27}	0.0	0.0	-4.47129×10^{-20}
A_4	1.05838×10^{-18}	0.0	8.07309×10^{-11}	3.89667×10^{-14}
A_2	1.42643×10^{-9}	-1.75666×10^{-6}	-1.18530×10^{-4}	-1.00590×10^{-8}
C	3.41621	6.74524	68.44582	3.41782
B_2	-34.48103	-2.35655×10^6	-1.58031×10^7	-44.46299
B_4	0.0	7.39436×10^{11}	1.43557×10^{12}	0.0
B_6	0.0	-8.68186×10^{16}	0.0	0.0
R	2.0×10^{-5}	3.0×10^{-5}	9.0×10^{-5}	1.1×10^{-4}

Table IV: Parameters of the approximation of ^{29}Si single crystal refractive index

Parameter	Spectral range			
	9400...730 cm^{-1} (1.06...13.70 μm)	730...617 cm^{-1} (13.70...16.21 μm)	617...573 cm^{-1} (16.21...17.45 μm)	573...114 cm^{-1} (17.45...85.72 μm)
A_6	4.16405×10^{-27}	0.0	0.0	0.0
A_4	1.03238×10^{-18}	0.0	1.45163×10^{-10}	4.61074×10^{-15}
A_2	1.42694×10^{-9}	-1.35827×10^{-6}	-2.03966×10^{-4}	-5.60442×10^{-10}
C	3.41588	5.89678	110.64230	3.41637
B_2	-29.06141	-1.69322×10^6	-2.49974×10^7	7.04348
B_4	0.0	5.12630×10^{11}	2.18071×10^{12}	-7.25535×10^5
B_6	0.0	-5.81255×10^{16}	0.0	0.0
R	2.0×10^{-5}	3.0×10^{-5}	1.0×10^{-4}	1.0×10^{-4}

Table V: Parameters of the approximation of ^{30}Si single crystal refractive index

Parameter	Spectral range			
	9310...720 cm^{-1} (1.07...13.89 μm)	720...605 cm^{-1} (13.89...16.53 μm)	605...565 cm^{-1} (16.53...17.70 μm)	565...112 cm^{-1} (17.70...89.29 μm)
A_{10}	0.0	1.58348×10^{-28}	0.0	0.0
A_8	0.0	-3.70584×10^{-22}	0.0	0.0
A_6	3.87178×10^{-27}	3.45410×10^{-16}	0.0	-5.25168×10^{-21}
A_4	1.06782×10^{-18}	-1.60314×10^{-10}	1.37221×10^{-10}	1.67675×10^{-14}
A_2	1.42449×10^{-9}	3.70631×10^{-5}	-1.87828×10^{-4}	-6.42102×10^{-9}
C	3.41535	0.0	99.59448	3.41676
B_2	-50.69159	0.0	-2.18377×10^7	-43.76842
B_4	0.0	0.0	1.85529×10^{12}	0.0
R	2.0×10^{-5}	3.0×10^{-5}	5.0×10^{-5}	1.0×10^{-4}

Table VI: Parameters of the approximation of $^{\text{nat}}\text{Si}$ single crystal refractive index

Parameter	Spectral range			
	9480...745 cm^{-1} (1.06...13.42 μm)	745...625 cm^{-1} (13.42...16.00 μm)	625...583 cm^{-1} (16.00...17.15 μm)	583...125 cm^{-1} (17.15...80.00 μm)
A_6	3.85272×10^{-27}	0.0	0.0	0.0
A_4	1.08707×10^{-18}	0.0	1.06100×10^{-10}	1.10503×10^{-14}
A_2	1.42510×10^{-9}	-1.38069×10^{-6}	-1.54334×10^{-4}	-4.28163×10^{-9}
C	3.41618	6.01658	87.37999	3.41725
B_2	-96.96621	-1.82986×10^6	-2.02501×10^7	-51.15422
B_4	0.0	5.71062×10^{11}	1.82698×10^{12}	-1.93263×10^5
B_6	0.0	-6.67343×10^{16}	0.0	0.0
R	2.0×10^{-5}	2.0×10^{-5}	6.0×10^{-5}	1.3×10^{-4}

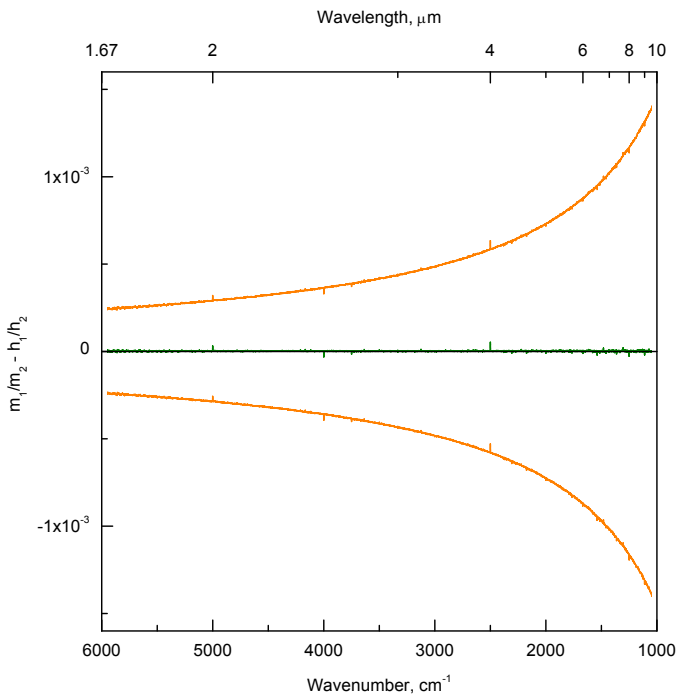


Figure 5: Spectral dependence of the left side of equation 3 for optimal and differing by ± 1 values of $m_{1,2}$.

where $\alpha_0 = \text{const}$, $\beta_0 = \text{const}$.

Thus, with Si atomic mass increasing, the electronic absorption edge shifts to shorter wavelengths, and the phonon absorption edge shifts to longer wavelengths. As a result, the dispersion curve of the refractive index in the transmission window should shift downwards without considerable changes in shape, as observed in our experiments.

VI. ACCURACY ANALYSIS

To measure the refractive index precisely by interference refractometry, the orders, m , of interference maxima should be determined with absolute accuracy. For this purpose we used the relation following from expression (1) written for two samples of different thickness, h_1 and h_2 , with interference orders $m_1(\nu)$ and $m_2(\nu)$, respectively:

$$\frac{m_1(\nu)}{m_2(\nu)} - \frac{h_1}{h_2} = \text{const} \quad (3)$$

If sample thickness is known with absolute accuracy, the constant in the right side of this equation turns to zero for a certain relation between $m_1(\nu)$ and $m_2(\nu)$. However, usually the sample thickness can be measured with some finite accuracy resulting in non-zero value of this constant [16]. Moreover, if the transmission spectra of the samples of different thickness are measured at different temperatures, spectral dependence of the left side

of equation (3) will be affected by the temperature dependence of the refractive index of a material. However, if one makes a wrong choice of the maxima orders at least by 1, the spectral dependence of the left side of equation (3) will explicitly differ from constant as evident from Fig. 5 for two $^{\text{nat}}\text{Si}$ samples.

Minimization of the right side of dependence (3) allows us to determine uniquely the maxima orders for each pair of samples. Additionally, the procedure of interference orders determination becomes simpler if the formula (1) is considered to be valid not only for the maxima but as well for all other points of the spectral transmission curve for which $m(\nu)$ values are not integer. One should use a linear approximation for $m_{1,2}$ frequency dependence in the interval between two nearest maxima (according to our calculations such an approximation is valid with the accuracy about 10^{-6} for $1 \dots 3 \text{ cm}^{-1}$ distance between the maxima) and increase the corresponding order by 1 passing over the next maximum. In this case the application of the (1) criterion becomes a simple search of orders corresponding to a given frequency in the transmission spectra of sample pairs, since the set of frequency values is the same for all spectra.

In the method of interference refractometry the error of the refractive index calculation depends on determination errors of all the variables occurring in the formula (1). If Fourier-transform spectrometer with the wavenumber precision better than 0.01 cm^{-1} is used, this error is mostly contributed by the sample thickness measurement error, Δh . The corresponding error in silicon refractive index is equal to $\Delta n = -n\Delta h/h$. If $\Delta h = 0.05 \text{ }\mu\text{m}$ and values of m are determined precisely for all interference maxima, one gets $\Delta n \approx 2 \times 10^{-4}$ on average for the only $\sim 1 \text{ mm}$ -thick sample used.

Using of two and more samples allows us to reduce this error due to the correlation of the refractive index values determined for all samples over the entire measurement range. Assuming the refractive index values to be identical for all the samples within the entire measurement range, we can analyze the influence of accuracy of the used thickness values on the final result of measurements and "correct" these thickness values. Analysis of the discrepancy between the "corrected" and initially used thicknesses provides an idea of how well the samples are prepared and measurements are made. Correction of thickness values (h_i , $i = 1, 2, 3$ in the case of three samples) is performed by orthogonal projecting in the (h_1, h_2, h_3) space the point with coordinates equal to these thickness values on a straight line representing solution of the following set of equations for all pairs of samples

$$\frac{h_1}{h_2} - \frac{m_1}{m_2} = 0, \quad \frac{h_1}{h_3} - \frac{m_1}{m_3} = 0, \quad \frac{h_2}{h_3} - \frac{m_2}{m_3} = 0$$

The refractive index values scatter, Δn_i , for sample of thickness h_i is obtained immediately from the relation

$$\Delta n_i = -n_i \frac{\Delta h_i}{h_i}$$

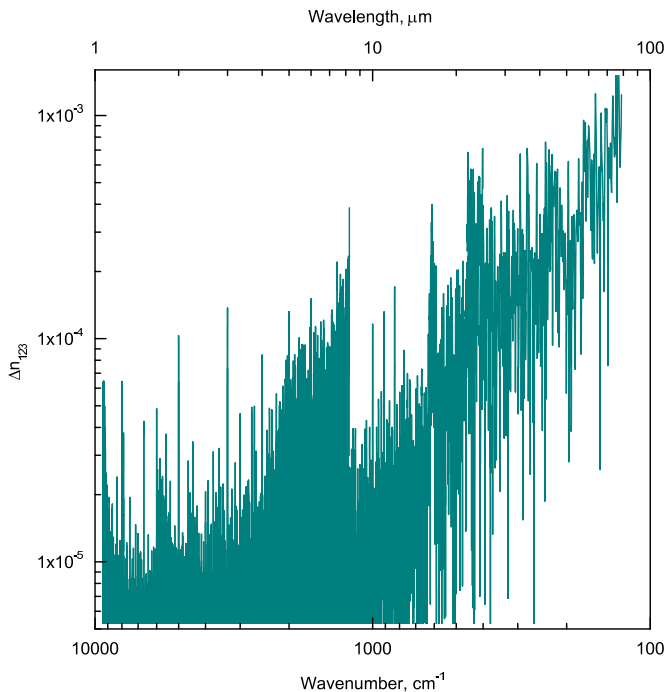


Figure 6: Spectral dependence of the difference Δn_{123} averaged between refractive index for ^{28}Si samples of different thicknesses.

where n_i is the "averaged" refractive index value, Δh_i is the difference between the "corrected" and initial thickness.

Table VII lists sample thickness measured on submicrometer at 21.2 °C and the thickness values corrected using the interference spectra in the middle ("MIR", from 2 to 25 μm) and near ("NIR", from 1.06 to 2 μm) infrared ranges, as well as the corresponding difference between the calculated and measured thicknesses. As is seen from Table VII the thickness correction value turns out to be extremely small for most of the samples not exceeding the error of direct measurement of the thickness. We estimate the average error of the refractive index determination resulting from the error of the samples thickness determination to be 1.3×10^{-4} . The contribution of the remaining factors influencing the samples transmission spectra measurements and, accordingly, our calculation of the refractive index performed similarly to paper [31], is found to be 10 times less and therefore is negligible.

Unlike the errors of thickness measurement and interference maxima orders determination, the error of the maxima positions determination is the only one exhibiting distinct frequency dependence: the latter error grows with the frequency decreasing (wavelength increasing) or in the absorption band vicinity and near the transparency range edges if any in the transmission spectra. To determine the maxima positions more exactly we restricted the range of the sample thicknesses used and spectrometer resolution to get not less than 20 experimental points

Table VII: Measured and corrected thicknesses of Si samples (in μm ; $i = 1, 2, 3$)

	h_i (measured)	h_i^{corr} (MIR)	h_i^{corr} (NIR)	Δh_{MIR}	Δh_{NIR}
^{28}Si	815.87	815.98	815.99	0.11	0.12
	1003.25	1003.23	1003.23	-0.02	-0.02
	1179.09	1179.03	1179.02	-0.06	-0.07
^{29}Si	815.95	815.98	815.98	0.03	0.03
	1003.23	1003.21	1003.23	-0.02	0.0
	1179.24	1179.23	1179.22	-0.01	-0.02
^{30}Si	816.09	816.12	816.13	0.03	0.04
	1003.34	1003.41	1003.38	0.07	0.04
	1179.54	1179.46	1179.48	-0.08	-0.06
$^{\text{nat}}\text{Si}$	815.87	815.88	815.88	0.01	0.01
	1003.27	1003.28	1003.28	0.01	0.01
	1179.15	1179.14	1179.14	-0.01	-0.01

between adjacent maxima in the corresponding transmission spectra. To estimate the influence of error of the maxima positions determination on the refractive index calculation, we determined the averaged difference between the refractive index values calculated for samples with different thickness. As an example, such a difference is presented in Fig. 6 for ^{28}Si samples.

VII. SUMMARY

In this work we have prepared and characterized high-purity single crystals of silicon stable isotopes, ^{28}Si , ^{29}Si , and ^{30}Si with enrichment above 99.9 at.%, and of silicon with natural isotopic composition, $^{\text{nat}}\text{Si}$. For the first time the spectral dependences of the refractive index of all single crystals are measured in wide transparency range from 1.06 to about 80 μm including the phonon absorption region.

The results of our study prove the refractive index values of mono-isotopic silicon single crystals to differ considerably. This may provide a possibility of manufacture of multilayer wave-guiding and quantum-sized structures operating in the IR spectrum range from different silicon isotopes to solve various problems of electronics and fiber and integrated optics.

ACKNOWLEDGMENTS

We are grateful to I. D. Kovalev and A. M. Potapov for determining the isotopic and chemical compositions of isotopically enriched silicon single crystals.

This work was supported by the Russian Foundation for Basic Research (grants No. 08-02-00964-a and No. 09-03-9741-R.Povolzh'e_a), by the Russian Federation President's Grants Council for Support to the Leading Scientific Schools of Russia (Grant

No. NSh-4701.2008.3) and by the Presidium of the Russian Academy of Sciences basic research projects "Novel

Optical Materials" and "Principles of Basic Research in Nanotechnologies and Nanomaterials".

-
- [1] P.T.Greenland, S.A.Lynch, A.F.G.vanderMeer, B.N.Murdin, C.R.Pidgeon, B.Redlich, N.Q.Vinh, and G.Aeppli, *Nature* 465, 1057 (2010)
- [2] V.G.Plotnichenko, V.O.Nazaryants, E.B.Kryukova, V.V.Koltashev, V.O.Sokolov, A.V.Gusev, V.A.Gavva, M.F.Churbanov, and E.M.Dianov, *Quantum Electron.* 40, 753 (2010).
- [3] G.G.Devyatykh, E.M.Dianov, A.D.Bulanov, O.Yu.Troshin, V.V.Balabanov, and D.A.Pryakhin, *Doklady Chemistry* 391, 204 (2003)
- [4] M.F.Churbanov, A.D.Bulanov, A.P.Kotkov, A.M.Potapov, O.Yu.Troshin, A.Yu.Loshkov, N.D.Grishnova, and S.A.Adamchik, *Doklady Chemistry* 432, 126 (2010)
- [5] A.V.Gusev and V.A.Gavva, Russian Federation Patent No.2370576 from 20.10.2009
- [6] J.R.Rosman and P.D.Taylor, *Pure Appl. Chem.* 70, 217 (1998)
- [7] I.D.Kovalev, A.M.Potapov, and A.D.Bulanov, *Mass spectrometry* 1, 37 (2004)
- [8] K.M.Itoh, J.Kato, M.M.Uemura, A.K.Kaliteevskii, O.N.Godisov, G.G.Devyatykh, A.D.Bulanov, A.V.Gusev, I.D.Kovalev, P.G.Sennikov, H.J.Pohl, N.V.Abrosimov, and H.Riemann, *Jpn. J. Appl. Phys.* 42, 6248 (2003)
- [9] J.W.AgerIII, J.W.Beeman, W.L.Hansen, E.E.Haller, I.D.Sharp, C.Liao, A.Yang, M.W.L.Thewalt, and H.Riemann, *J.Electrochem. Soc.* 152, G448 (2005)
- [10] I.D.Kovalev, K.N.Malyshev, A.M.Potapov, and A.I.Suchkov, *J. Analytical Chem.* 56, 437 (2001)
- [11] *Annual Book of ASTM Standards*, vol.10.05 Electronics(II), 1996
- [12] M.Cardona and M.L.W.Thewalt, *Rev. Modern Phys.* 77, 1173 (2005)
- [13] P.G.Sennikov, T.V.Kotereva, A.G.Kurganov, B.A.Andreev, H.Niemann, D.Schiel, V.V.Emtsev, and H.-J.Pohl, *Semiconductors* 39, 320 (2005)
- [14] A.V.Vasil'ev, V.V.Voitsekhovskii, and V.G.Plotnichenko, *High-Purity Subst.* 3, 39 (1991) (in Russian)
- [15] V.G.Plotnichenko, V.O.Nazaryants, E.B.Kryukova, and E.M.Dianov, *J. Physics D: Applied Physics* 43, 105402 (2010)
- [16] V.O.Nazaryants, E.B.Kryukova, E.M.Gavrishchuk, V.B.Ikonnikov, S.M.Mazavin, and V.G.Plotnichenko, *Appl. Optics* 49, 4723 (2010)
- [17] H.B.Briggs, *Phys. Rev.* 77, 286 (1950)
- [18] C.D.Salzberg and J.J.Villa, *J. Opt. Soc. Am.* 47, 244 (1957)
- [19] H.H.Li, *J. Phys. Chem. Ref. Data* 9, 561 (1980)
- [20] D.F.Edwards and E.Ochoa, *Appl. Optics* 19, 4130 (1980)
- [21] B.J.Frey, D.B.Leviton, and T.J.Madison, *Proc. SPIE* 6273, 62732J (2006)
- [22] V.G.Plotnichenko, V.O.Nazaryants, E.B.Kryukova, Yu.N.Pyrkov, E.M.Dianov, B.I.Galagan, and S.E.Sverchkov, *Inorg. Mater.* 45, 322 (2009)
- [23] D.Y.Smith, M.Inokuti, and W.Karstens, *J. Phys.: Condens. Matter.* 13, 3883 (2001)
- [24] U.Fano, *Phys. Rev.* 118, 451 (1960)
- [25] V.M.Agranovich and V.L.Ginzburg, *Crystal Optics with Spatial Dispersion and Excitons*, Springer-Verlag, Berlin, 1984, 441p.
- [26] M.Cardona, *phys. stat. sol. (b)* 220, 5 (2000)
- [27] L.F.Lastras-Martinez, T.Ruf, M.Konuma, M.Cardona, and D.E.Aspnes, *Phys. Rev. B* 61, 12946 (2000)
- [28] A.K.Ramdas, S.Rodriguez, S.Tsoi, and E.E.Haller, *Solid State Communications* 133, 709 (2005)
- [29] C.P.Herrero, *Solid State Communications* 110, 243 (1999)
- [30] K.Winer and M.Cardona, *Phys. Rev. B* 35, 8189 (1987)
- [31] R.Gupta and S.G.Kaplan, *J. Res. Natl. Inst. Stand. Technol.* 108, 429 (2003)